

Influence of Infill Design in Fabrication of 3D-printed PLA Parts Using FDM

Tamilanban THANGARAJU¹, Pankaj KUMAR²,
Dhanesh Babu SAMUEL DHANASEKARAN³, Ganesh Babu LOGANATHAN⁴,
Bhavya PAPE GOWDA⁵, Thenmozhi SIVAKUMAR⁶, Nafeez Ahmed LIYAKAT^{7*}

¹ Department of Mechanical Engineering, St. Joseph College of Engineering, Chennai-602117, India

² Department of Mechanical Engineering, GMR Institute of Technology, Rajam-532127, Andhra Pradesh, India

³ Department of Mechanical Engineering, Chennai Institute of Technology, Chennai-600069, Tamil Nadu, India

⁴ Department of Robotics and Automation, Rajalakshmi Engineering College, Chennai-602105, India

⁵ Department of Applied Sciences- Physics, New Horizon College of Engineering, Bangalore-560103, India

⁶ Department of Aeronautical Engineering, Gojan School of Business and Technology, Chennai-600052, India

⁷ Department of Mechanical and Automation Engineering, Gojan School of Business and Technology, Chennai-600052, India

<http://doi.org/10.5755/j02.ms.38235>

Received 29 July 2024; accepted 16 September 2024

The present work examines the mechanical characteristics of polylactic acid (PLA) samples manufactured in 3D printing using various infill patterns. The infill patterns investigated are cuboid, grid, and octet, prepared at a constant infill density of 50 %. The study aimed to identify the most suitable infill pattern for specific mechanical requirements, considering tensile, compression, and flexural behaviour. Experimental testing was conducted on the 3D-printed PLA specimens to assess their mechanical performance. The findings reveal that the octet infill pattern showed the highest mechanical qualities across all three tests, including tensile, flexural, and compression evaluations, indicating improved strength and stability. The octet infill pattern samples had the highest tensile value of 17.3 MPa, maximum flexural stress of 35 MPa, and maximum compression stress of 34.4 MPa. These results emphasize the need to choose suitable infill patterns to adjust the mechanical properties of 3D-printed PLA components to meet particular application requirements.

Keywords: additive manufacturing, FDM, 3D-printing, PLA, infill pattern, infill density.

1. INTRODUCTION

The layer-by-layer construction of 3D materials using Additive Manufacturing (AM) is essential for industrial and other applications. Several sectors, including aerospace, automotive, marine, medical, and defence, use additive manufacturing. [1–3]. Materials are produced using the AM technique known as fused deposition modelling (FDM), also referred to as fused filament fabrication (FFF). FDM has gained much popularity since it is simpler and less expensive than other three-dimensional printing techniques. The primary advantages of FDM are its low price, simplicity, usefulness as a training tool, and quick model development [4, 5]. In FDM, several different variables can affect the mechanical characteristics of produced products. The following elements play a major role in achieving precision: build orientation, layer thickness, nozzle heat, nozzle diameter, bed temperature, infill structure, infill density, and printing rate. Raster angle, air gap, raster width, and wire width are other factors that affect the mechanical and aesthetic aspects of the surface. FDM is a process that may undoubtedly produce samples more rapidly and inexpensively, but there have also been certain issues with the technique that should be taken into account [6].

An aliphatic polyester thermoplastic called polylactic acid (PLA) is made from maize and sugarcane starches.

Since 3D printing does not require a heated surface for the objects being printed, PLA has a low glass transition temperature ($T_g = 60–65\text{ }^\circ\text{C}$) and melting temperature ($T_m = 173–178\text{ }^\circ\text{C}$) [7]. The strength of the products is significantly influenced by the type of support, layer thickness, and material infill [8]. The infill is the inside framework of a 3D-printed component. There are a variety of infill patterns that may be employed, and each one performs a specific task and possesses a particular set of mechanical properties, including toughness and rigidity. The most typical forms of infill patterns include grids, triangular, hexagonal, linear, and others. Infill density is equally important for the mechanical properties of 3D-printed items as infill constructions. It has been observed that by raising the infill density, the mechanical characteristics, tensile strength, and flexural strength are all enhanced [9]. Infill density is a key influence in weight reduction, which, when combined with materials that have high stiffness and strength, allows for the creation of some useful structures [10, 11].

The presence of gaps in the sample will depend on the printing circumstances, which will ultimately affect the mechanical properties of the final product [12]. Eryildiz [1] evaluated the influence of several infill patterns (3D honeycomb, stars, gyroid, honeycomb, and Hilbert curve) on the mechanical characteristics of PLA objects produced

* Corresponding author; N.A. Liyakat
E-mail: nafeezahmed.1@gojaneducation.com

via 3D printing. The findings revealed that the honeycomb infill pattern had the best mechanical characteristics. Chicco et al. [13] examined how the infill density (25, 50, 75, and 100 %) of samples composed of poly (lactic acid) (PLA) reinforced with short glass fibres (GF) manufactured using the FFF technique affects the mechanical and thermal response of the materials. The findings indicated that the infill density of the additive-manufactured samples improved with an increase in tensile, flexural, and compression strength; as a result, samples with 100% infill density provided the strongest mechanical characteristics. Cwika et al. [14] demonstrated how the mechanical properties of samples created by AM utilizing the FFF are influenced by the solid layers, infill density, and infill pattern. Increased infill percentage was shown to lessen distortion, and the thickness of the shell had a significant impact on tensile strength, according to the scientists.

The tensile fracture behaviour of 3D-printed PLA parts is influenced by several factors, including the printing parameters, infill density, layer orientation, and the inherent properties of the material itself. Previous studies have reported that the infill pattern plays a significant role in the tensile fracture behaviour of FDM 3D printed parts, with parts printed with higher density exhibiting the highest tensile strength. Additionally, the presence of defects, such as voids or delamination between layers, can lead to premature failure and reduced tensile strength [15]. Infill patterns with fewer air gaps and stronger layer bonding, such as the honeycomb pattern, exhibit improved fracture resistance during tensile tests. This is due to the increased contact area between material layers, which reduces the likelihood of delamination and premature failure [16]. Marşavina 2022 [17] examined the impact of manufacturing parameters on the mechanical properties of 3D-printed PLA parts. Findings revealed that specimen orientation, layer thickness, and filament colour significantly influence tensile strength and fracture behaviour. The fracture surfaces of 3D-printed ABS/TPE parts exhibited different morphologies based on build orientation. Parts built in the ZXY direction showed more cavities, likely due to layer interface failure. This correlated with lower mechanical strength compared to XYZ-built parts. However, the ABS/TPE system demonstrated potential for reducing anisotropy in 3D-printed components [18].

Cuboid, grid, and octet patterns are relatively easy to implement in most 3D printing software and hardware which is considered practically suitable. The selection of cuboid, grid, and octet infill patterns for 3D-printed PLA parts is based on a combination of factors, including previous research, comparative studies, and practical considerations. The cuboid pattern is chosen for its simplicity and predictability, the grid for its balanced strength and material efficiency, and the octet for its superior strength-to-weight ratio, especially in high-performance applications. These patterns represent a range of options that can be tailored to the specific needs of different 3D printing projects, as supported by numerous studies in the field [19].

This study examined the impact of infill design on FDM-printed PLA parts for 3D printing. The effects of various infill patterns on mechanical characteristics and general part performance through examination and testing

are investigated. Three infill patterns grids, octets, and cuboids are compared with respect to the mechanical qualities and functionality of 3D-printed PLA parts.

2. EXPERIMENTAL DETAILS

The Commercial PLA filament of 1.75 mm in diameter was utilized as the feedstock for a Creality CR 10 smart pro-3D printer with a 0.4 mm nozzle.

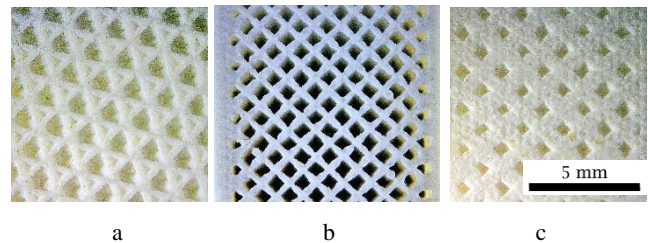


Fig. 1. 3D-printed infill pattern: a – cuboid; b – grid; c – octet

Table 1. Parameters of PLA

Material	PLA
Density	1.24 g/cm ³
Melting temperature	190–230 °C
Glass transition temperature	56–64 °C

Initially, the specimens were designed with CAD software, and the designed specimen models will be sliced using Creality slicer V 4.8 slicing software. Then, they will be converted into the Standard Triangular Language (STL) format, and finally, the STL file format will be inserted into the Creality CR 10 smart pro-3D printer. Fig. 2 shows the schematic illustration of a 3D printer used in our work. Then, sample pieces are fabricated as per the printer parameters mentioned in Table 1. Three different patterns and infill densities were used to build the specimens: cubic, grid, and octet, with an infill density of 50 %. Three 3D-printed infill patterns such as cuboid, grid, and octet are depicted in Fig. 1.

The specimens were printed using a 3D printer with a nozzle diameter of 0.4 mm at 0.15 mm layer thickness and 0.2 mm initial layer height. Throughout the whole printing process, the bed temperature was kept at 60 °C while the nozzle temperature was set to 210 °C. Since no contours were printed, the entire specimen typically consisted of 5 compact layers on top, 5 compact layers on the bottom, and pure infill in between, with overall dimensions of 20 mm × 20 mm × 20 mm.

The tensile testing of the specimen was carried out employing the highly sophisticated Z010 Proline Universal Testing Machine (UTM), equipped with a precision X-force K load cell and expertly designed pneumatic grips, in strict adherence to the revered ASTM D638 standard. The testing protocol encompassed subjecting the specimen to an initial pre-load of 0.1 MPa, followed by a continuous and controlled tensile loading rate of 1 mm/min, while concurrently imposing a displacement rate of 50 mm/min. For the subsequent flexural test, the Z010 Proline UTM. The controlled test speed of 10 mm/min was followed. Finally, the compression test, a vital aspect of material evaluation, was rigorously conducted using the Z010 Proline UTM. The test proceeded under a controlled test speed, ensuring precision and repeatability, set at 1.3 mm/min, while a pre-

defined pre-load of 0.1 MPa was applied to the specimen to facilitate proper contact and alignment. The mechanical tests were conducted according to the following ASTM standards: tensile – ASTM D638, flexural – ASTM D790, compression – ASTM D695. The fractured surfaces are analyzed using an optical microscope with 100^x magnification. For each mechanical test conducted, three specimens were tested. The average values of these three results were considered.

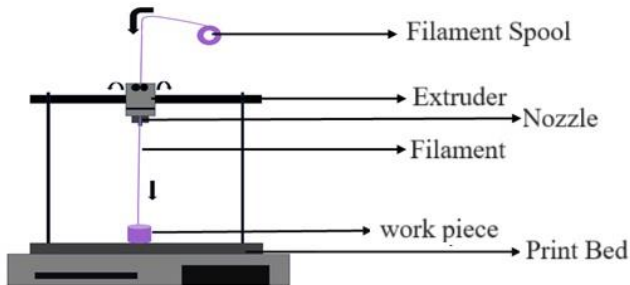


Fig. 2. Schematic representation of FDM 3D printer

3. RESULTS AND DISCUSSION

3.1. Tensile test analysis

Fig. 3 shows the tensile test specimen after the test. Table 2 shows the tensile strength and percentage elongation of the three infill patterns. The stress-strain diagram of octet, grid, and cuboid-infilled samples is shown in Fig. 4. The specimen with an octet infill pattern was shown to have the highest tensile value of 17.3 MPa when compared to specimens with grid and cuboid infill patterns, which are 14.8 MPa and 10.2 MPa, respectively. The octet pattern's exceptional surface bonding, which led to improved load transfer mechanisms and stronger interlayer adhesion, is responsible for its outstanding tensile qualities. On the other hand, the grid infill pattern had the lowest tensile characteristics because of poor surface bonding, which lowered its load-bearing capacity. Additionally, raster spacing and inter-raster bonding are significant factors in influencing the specimen's tensile strength [20].

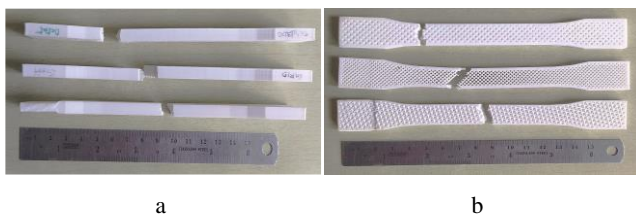


Fig. 3. 3D printed samples after the tensile test: a – side view; b – front view

The octet allows for more constant bonding within the layers and causes greater inter-raster bonding with a small raster gap. In the grid infill pattern specimen, in each layer, there are lines arranged in both diagonal directions. Because of this, the 3D-printed samples show weak inter-raster bonding and a huge raster gap, which results in less tensile strength. According to the fracture analysis, all three tensile specimens showed fracture due to brittle mode. The fracture analysis of tensile failure is shown in the Fig. 5. The

specimens crack at different points, which may be due to the impact of layer bonding and orientation of the infill pattern. The existence of air gaps in the cuboid pattern, which led to quick fracture during the test, was also blamed for the drop in mechanical properties. The mechanical qualities of PLA items created using 3D printing technology could be impacted by air gaps as well as layer adhesion strength.

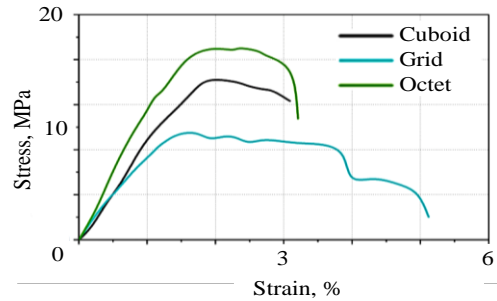


Fig. 4. Stress-strain diagram of the octet, grid, and cuboid-infilled samples

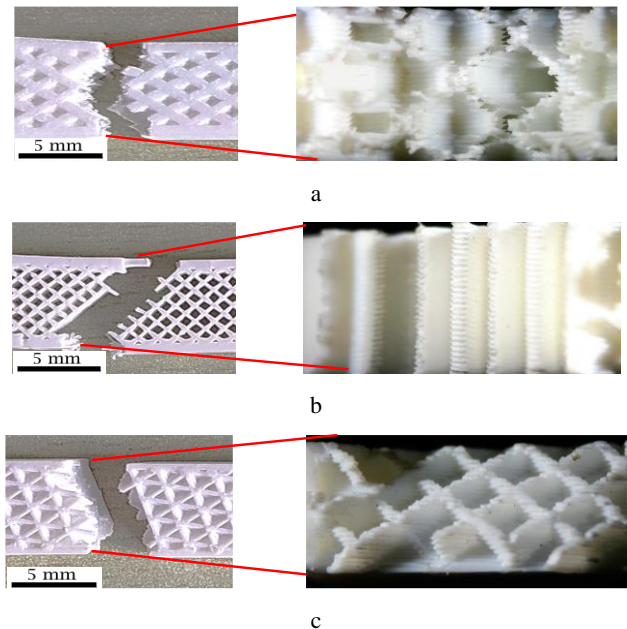


Fig. 5. Fracture analysis of tensile failure

The octet infill pattern reduces air gaps in 3D components, allowing the material layers and filaments to adhere more securely and raising the PLA molecular chain's resistance.

3.2. Flexural test analysis

The 3D printed specimens after the flexural test are shown in Fig. 6, and Fig. 7 illustrates the stress-strain diagram of an octet, grid, and cuboid infilled samples.

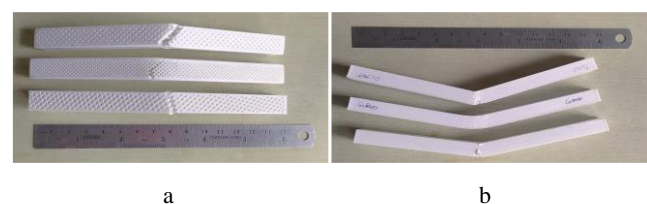


Fig. 6. 3D printed specimens after the flexural test

The specimen with an octet design exhibited the highest flexural properties when compared to specimens with grid and cuboid infill patterns, according to the findings of the flexural test, which was carried out at a rate of 10 mm/min. Better flexural strength, or greater deformation when subjected to bending forces, was demonstrated by the octet pattern.

Contrarily, the cuboid infill pattern had the lowest flexural strength, which was primarily a result of its compromised structural integrity and susceptibility to deformation. These results, which highlight how infill patterns affect specimen flexural behaviour, aid in enhancing the performance of materials in pertinent applications.

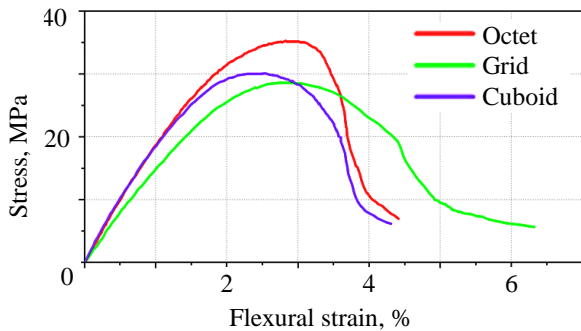


Fig. 7. Stress-strain diagram of octet, grid, and cuboid infilled samples

Flexural fracture analysis (Fig. 8) reveals that all three specimens showed a brittle mode of fracture.

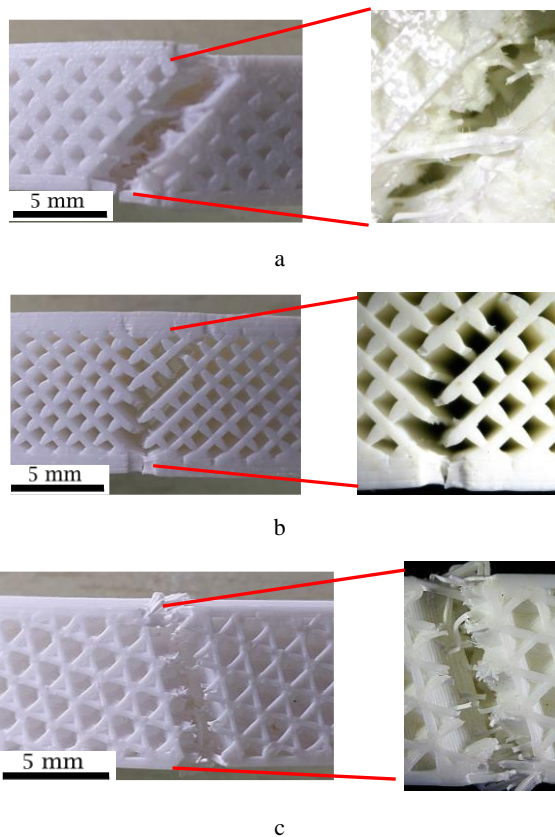


Fig. 8. Fracture analysis of flexural failure

According to Aloyaydi et al.,[4] specimens prepared with less infill density showed a brittle mode of fracture during flexural tests. Raising the infill density increased the propensity for ductile fracture at the cost of brittle fracture mode. These results can be related to the fact that samples with 50 % infill density have a substantial volume proportion of porosity, which caused the samples to be more brittle and less deformable. As a result, the major mechanism that occurred here was brittle failure. Octet infill demonstrates superior mechanical performance due to its interconnected structure and efficient load distribution. The lower flexural strength of the cuboid infill pattern is primarily due to its geometric weakness, limited interlocking, reduced bonding area, higher void volume, and potential stress concentration. Grid infill offers intermediate performance due to its interconnected structure.

3.3. Compression test analysis

The compression test was conducted at the rate of 1.3 mm/min, and the test samples after the compression test are shown in Fig. 9.

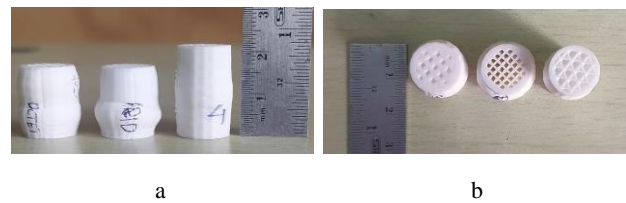


Fig. 9. Specimens after the compression test

All the specimens buckled under the axial pressure. Double paralleling was visible at the top and bottom surfaces of the specimen with the octet infill pattern, whereas only single buckling was visible in the centre of the specimen with the grid and cuboid infill patterns. Compared to other specimens, the cuboid infill pattern demonstrated the least buckling. The specimen with lesser rigidity fails as a result of buckling. The stress-strain graph from the compression analysis is shown in Fig. 10. Table 3 represents the compression test analysis of the various infill patterns.

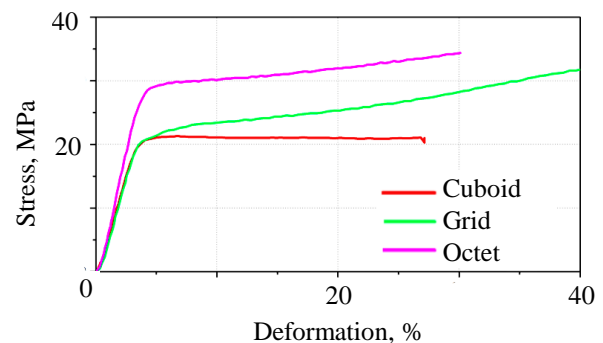


Fig. 10. Stress-strain analysis of compression test

The octet infill pattern sample had a maximum compression stress of 34.4 MPa and a deformation of 30 %, whereas the grid infill sample's compressive behaviour produced a minimum stress of 32 MPa and a sizable displacement of 40 %. The cuboid sample, in comparison, showed a maximum stress of 21.3 MPa and a relatively small deformation of 6.6 %. The observed results show that the grid infill sample failed due to considerable distortion,

whereas the cuboid sample failed due to minimal deformation before the failure. The octet infill pattern generally demonstrated a higher maximum compressive stress compared to the cuboid pattern, indicating greater strength and resistance to compression. This can be attributed to the geometric complexity and load-distributing characteristics of the octet structure. Regarding deformation, the octet pattern also exhibited less deformation at maximum stress levels compared to the cuboid pattern. The inherent stability and uniform distribution of forces within the octet structure contribute to its lower deformation under load, making it a more efficient infill pattern for applications requiring high compressive strength and minimal deformation.

4. CONCLUSIONS

This study investigated the mechanical properties of 3D-printed PLA (Polylactic Acid) specimens with varying infill patterns, specifically cuboid, grid, and octet, all set at a uniform infill density of 50 %. The results are as follows. The octet infill pattern specimen showed the highest tensile value of 17.3 MPa when compared to specimens with grid and cuboid infill patterns. The octet pattern's exceptional surface bonding, which led to improved load transfer mechanisms and stronger interlayer adhesion, is responsible for its outstanding tensile qualities. All tensile failure results show that a brittle mode of failure was observed.

The highest flexural strength of 35 MPa was observed in the Octet infill pattern specimen. The grid infill pattern had the lowest flexural strength of 28 MPa, which was primarily a result of its compromised structural integrity and susceptibility to deformation. Flexural failure fracture analysis reveals that a brittle mode of fracture was seen in every specimen. Air gaps and layer adhesion strength may have an impact on the failure of the PLA specimens.

All three specimens buckled under axial stress during the compression test, and the octet infill pattern exhibits the greatest compressive strain (34.4 MPa), followed by the grid pattern (32 MPa). According to the observed data, the cuboid sample (21.3 MPa) failed due to very little deformation prior to the failure, in contrast to the other sample, due to significant distortion.

REFERENCES

1. **Eryildiz, M.** The Effects of Infill Patterns on the Mechanical Properties of 3D Printed PLA Parts Fabricated by FDM *Ukrainian Journal of Mechanical Engineering and Materials Science* 7 2021: pp. 1–8. <https://doi.org/10.23939/ujmems2021.01-02.001>
2. **Birosz, M.T., Ledenyak, D., Ando, M.** Effect of FDM Infill Patterns on Mechanical Properties *Polymer Testing* 113 2022: pp. 107654. <https://doi.org/10.1016/j.polymertesting.2022.107654>
3. **Pernet, B., Nagel, J.K., Zhang, H.** Compressive Strength Assessment of 3D Printing Infill Patterns *Procedia CIRP* 105 2022: pp. 682–687. <https://doi.org/10.1016/j.procir.2022.02.114>
4. **Aloyaydi, B., Sivasankaran, S., Mustafa, A.** Investigation of Infill Patterns on Mechanical Response of 3D Printed Poly-Lactic-Acid *Polymer Testing* 87 2020: pp. 106557. <https://doi.org/10.1016/j.polymertesting.2020.106557>

5. **Mohamed, O.A., Masood, S.H., Bhowmik, J.L.** Optimization of Fused Deposition Modeling Process Parameters: A Review of Current Research and Future Prospects *Advances in Manufacturing* 3 2015: pp. 42–53. <https://doi.org/10.1007/s40436-014-0097-7>
6. **Lalegani Dezaki, M., Mohd Ariffin, M.K.A.** The Effects of Combined Infill Patterns on Mechanical Properties In FDM Process *Polymers* 12 (12) 2020: pp. 2792. <https://doi.org/10.3390/polym12122792>
7. **Fehri, S., Cinelli, P., Coltelli, M.B., Anguillesi, I., Lazzeri, A.** Thermal Properties of Plasticized Poly (Lactic Acid) (PLA) Containing Nucleating Agent *International Journal of Chemical Engineering and Applications* 7 (2) 2016: pp. 85–88. <https://doi.org/10.7763/IJCEA.2016.V7.548>
8. **Ganesh Kumar, S., Kumar, S.D., Magarajan, U., Rajkumar, S., Arulmurugan, B., Sharma, S., Li, C., Ilyas, R.A., Badran, M.F.** Investigation of Tensile Properties of Different Infill Pattern Structures Of 3D-Printed PLA Polymers: Analysis and Validation Using Finite Element Analysis in ANSYS *Materials* 15 (15) 2022: pp. 5142. <https://doi.org/10.3390/ma15155142>
9. **Camargo, J.C., Machado, A.R., Almeida, E.C., Silva, E.F.** Mechanical Properties of PLA-Graphene Filament for FDM 3D Printing *International Journal of Advanced Manufacturing Technology* 103 2019: pp. 2423–2443. <https://link.springer.com/article/10.1007%2Fs00170-019-03532-5>
10. **Fores Garriga, A., Perez, M.A., Gomez-Gras, G., Reyes-Pozo, G.** Role of Infill Parameters on the Mechanical Performance and Weight Reduction of PEI Ultem Processed by FFF *Materials & Design* 193 2020: pp. 108810. <https://doi.org/10.1016/j.matdes.2020.108810>
11. **Hu, H., Qin, Q.H.** Advances in Fused Deposition Modeling of Discontinuous Fiber/Polymer Composites *Current Opinion in Solid State and Materials Science* 24 (5) 2020: pp. 100867. <https://doi.org/10.1016/j.cossms.2020.100867>
12. **Keat, Y.C., Yin, Y.W., Ramli, M.Z., Leng, T.P., Chie, S.C.** Effects of Infill Density on the Mechanical Properties Of 3D Printed PLA And Conductive PLA *AIP Conference Proceedings* 2129 (1) 2019: pp. 020013-1-4. <http://dx.doi.org/10.1063/1.5118021>
13. **Chicos, L.A., Pop, M.A., Zaharia, S.M., Lancea, C., Buican, G.R., Pascariu, I.S., Stamate, V.M.** Fused Filament Fabrication of Short Glass Fiber-Reinforced Polylactic Acid Composites: Infill Density Influence on Mechanical and Thermal Properties *Polymers* 14 (22) 2022: pp. 4988. <https://doi.org/10.3390/polym14224988>
14. **Cwikla, G., Grabowik, C., Kalinowski, K., Paprocka, I., Ociepa, P.** The Influence of Printing Parameters on Selected Mechanical Properties of FDM/FFF 3D-Printed Parts *IOP Conference Series: Materials Science and Engineering* 227 (1) 2017: pp. 012033. <http://dx.doi.org/10.1088/1757-899X/227/1/012033>
15. **Fuentes, M.A., Thakur, S., Wu, F., Misra, M., Gregori, S., Mohanty, A.K.** Study on the 3D Printability of Poly(3-Hydroxybutyrate-Co-3-Hydroxyvalerate)/Poly (Lactic Acid) Blends with Chain Extender Using Fused Filament Fabrication *Scientific Reports* 2020. pp. 11804. <https://doi.org/10.1038/s41598-020-68331-5>
16. **Eryildiz, M.** The Effects of Infill Patterns on The Mechanical Properties of 3D Printed PLA Parts Fabricated by FDM

Ukrainian Journal of Mechanical Engineering and Materials Science 7 (1–2) 2021: pp. 1–8.
<https://doi.org/10.23939/ujmems2021.01-02.001>

17. **Marşavina, L., Vălean, C., Mărghitaş, M., Linul, E., Razavi, N., Berto, F., Brighenti, R.** Effect of The Manufacturing Parameters on the Tensile and Fracture Properties of FDM 3D-Printed PLA Specimens *Engineering Fracture Mechanics* 274 2022: pp. 108766.
<https://doi.org/10.1016/j.engfracmech.2022.108766>
18. **Perez, A.R.T., Roberson, D.A., Wicker, R.B.** Fracture Surface Analysis of 3D-Printed Tensile Specimens of Novel ABS-Based Materials *Journal of Failure Analysis and Prevention* 14 (3) 2014: pp. 343–353.
<https://doi.org/10.1007/s11668-014-9803-9>
19. **Persad, J., Roche, S.** Impact of 3D Printing Infill Patterns on The Effective Permittivity of 3D Printed Substrates *In IEEE Journal of Microwaves* 4 (2) 2024: pp. 277–292.
<http://dx.doi.org/10.1109/JMW.2024.3369599>
20. **Kannan, S., Vezhavendhan, R., Kishore, S., Kanumuru, K.V.** Investigating the Effect of Orientation, Infill Density with Triple Raster Pattern on the Tensile Properties for 3D Printed Samples *IOP Science Notes* 1 (2) 2020: pp. 024405.
<http://dx.doi.org/10.1088/2633-1357/abb290>



© Thangaraju et al. 2025 Open Access This article is distributed under the terms of the Creative Commons Attribution 4.0 International License (<http://creativecommons.org/licenses/by/4.0/>), which permits unrestricted use, distribution, and reproduction in any medium, provided you give appropriate credit to the original author(s) and the source, provide a link to the Creative Commons license, and indicate if changes were made.